Journal of Thermal Analysis, Vol. 41 (1994) 493-509

In celebration of the 60th birthday of Dr. Andrew K. Galwey

COMPUTERIZED APPLICATION OF THE ZSAKÓ METHOD OF ANALYSIS

*P. P. Stander[1] and C. P. J. van Vuuren[2]**

[1]Mintek, Private Bag X3015, Randburg, 2125 South Africa
[2]Department of Materials Science and Metallurgical Engineering, University of Pretoria Pretoria, 0002 South Africa

Abstract

Kinetic parameters and mechanisms of solid state reactions can be determined from a single non-isothermal experiment using the Zsakó method. This method has been computerized and applied in theoretical and practical studies and in the separation of overlapping reactions.

Keywords: kinetics, Zsakó method

Introduction

The fundamental equation on which nearly all non-isothermal kinetic analyses [1–11] are based, can be written as

$$f(\alpha) = \frac{AE_a}{R\varphi} p(x) \tag{1}$$

or

$$\ln f(\alpha) - \ln p(x) = \ln \frac{AE_a}{R\varphi} = B \tag{2}$$

* Author to whom correspondenc should be addressed.

John Wiley & Sons, Limited, Chichester
Akadémiai Kiadó, Budapest

where

$$B = \ln \frac{AE_a}{R\varphi} \tag{3}$$

α is the fractional reaction
$f(\alpha)$ is the integral form of a kinetic model
A is the frequency factor in the Arrhenius equation
E_a is the activation energy of the reaction
R is the universal gas constant
φ is the linear heating rate to which the sample is subjected and

$$p(x) = \int_x^\infty \frac{e^{-x}}{x^2} dx \tag{4}$$

with

$$x = \frac{E_a}{RT} \tag{5}$$

The integral in Eq. (4) does not have an analytical solution, and numerous methods of evaluating this integral have been proposed [12].

Gyulai and Greenhow [11, 13], Coats and Redfern [14], Horowitz and Metzger [15] and MacCullum and Tanner [16] are but a few investigators who have used different methods to evaluate the integral $p(x)$, and have therefore provided different approaches to non-isothermal solid state kinetics.

There has been much discussion of the possibility of determining kinetic parameters, and especially mechanisms, from a single non-isothermal curve. As recently as 1988, Somasekharam and Kalpagham [17] stated that it is impossible to determine the mechanism from non-isothermal data and that isothermal measurements should be used to determine the mechanisms applicable to solid state reactions. Criado *et al.* [4] also stated that it is impossible to determine the kinetic description for a reaction from a single non-isothermal kinetic curve. In this study it is shown that, with the systematic approach used, the mechanisms of solid state reactions can be determined with relative ease and reasonable selectivity in contrast to the above statements.

Description of software

Software in Pascal was developed for IBM/XT or AT compatible microcomputers. The method used is based on the approach of Zsakó [18] with modifications and extensions introduced.

A kinetic curve of n observations, $\alpha_i T_i$, obtained from TG, DTA or DSC data collected at a constant heating rate (φ), serves as primary input. These data are compared to twenty well-established models (Table 1) in the following way:

Table 1 Kinetic models used in the present paper

Model number	$f(\alpha)$	Description
F1	α^2	Parabolic law, n=1/2
F2	$\alpha + (1-\alpha)\ln(1-\alpha)$	Valensi-Barrer
F3	$(1-\frac{2}{3}\alpha) - (1-\alpha)^{\frac{2}{3}}$	Ginstling-Brounstein
F4	$[1-(1-\alpha)^{\frac{1}{3}}]^2$	Jander
F5	$[(1+\alpha)^{\frac{1}{3}}-1]^2$	Anti-Jander
F6	$([1/(1-\alpha)]^{\frac{1}{3}}-1)^2$	Zhuralev-Lesokin-Tempelman
F7	$\ln[\alpha/(1-\alpha)]$	Prout-Tompkins
F8	$-\ln(1-\alpha)$	First-order
F9	$[-\ln(1-\alpha)]^{\frac{2}{3}}$	Avrami-Erofeev (n=1.5)
F10	$[-\ln(1-\alpha)]^{\frac{1}{2}}$	Avrami-Erofeev (n=2)
F11	$[-\ln(1-\alpha)]^{\frac{1}{3}}$	Avrami-Erfoeev (n=3)
F12	$[-\ln(1-\alpha)]^{\frac{1}{4}}$	Avrami-Erofeev (n=4)
F13	$1-(1-\alpha)^{\frac{1}{2}}$	Contracting-area
F14	$1-(1-\alpha)^{\frac{1}{3}}$	Contracting-volume
F15	α	Power law, n=1
F16	$\alpha^{\frac{1}{2}}$	Power law, n=2
F17	$\alpha^{\frac{1}{3}}$	Power law, n=3
F18	$\alpha^{\frac{1}{4}}$	Power law, n=4
F19	$(1-\alpha)^{-1}-1$	Second-order
F20	$(1-\alpha)^{-\frac{1}{2}}$	Third-order

Limits of an E_a calculation range, say $E_{a,1}$ and $E_{a,2}$ are determined by the values of T_1 and T_n and by using Eq. (5) and the limits of x. The value of E_a is

systematically varied between the limits $E_{a,1}$ and $E_{a,2}$. At every value of E_a between these two limits and with a specific choice of kinetic model, $f(\alpha)$, the procedure is as follows:

For every experimental observation, $\alpha_i T_i$, with $i \in [1,n]$, x is calculated according to Eq. (5), and $\ln p(x)$ by means of linear interpolation. The value of $f(\alpha)$ is calculated according to the specific model under consideration. The value of B (Eq. (2)) can therefore be calculated from the values of $f(\alpha)$ and $p(x)$ for every observation.

For the right choice of kinetic model $f(\alpha)$ and E_a, B should theoretically be constant for every observation α_i, T_i with $i \in [1,n]$. This implies that the standard deviation on the average value of B, say S_B, should be zero in this instance. S_B is a function of E_a and will ultimately have a global minimum at a specific value of E_a. The value of E_a at which S_B is a minimum is the E_a value leading to the best description of the experimental data by the specific model $f(\alpha)$ under consideration. The value of A can be calculated from the average value of B using the E_a value at which S_B is a minimum.

A table of E_a, A, $S_{B,min}$, α_{err} and $\alpha_{err,max}$ is constructed for all kinetic models. This table also shows whether S_B goes through a global minimum between the E_a calculation range limits. The optimum value of E_a is reported to the nearest 0.1 $kJ \cdot mol^{-1}$. This table enables selection of the model best describing the experimental data.

The minimum value of S_B, say $S_{B,min}$, is most probably the model which best describes the experimental kinetic curve and this model is therefore most applicable to the reaction and experimental conditions considered.

Non-isothermal curves are simulated using the determined optimum values of E_a and A for the kinetic model considered. Not only does this give a visual indication of how well the model describes experimental data, but by calculating the average error in α, say α_{err}, and the maximum error, say $\alpha_{err,max}$, the theoretical description of experimental data is quantified.

Using the defined parameters $S_{B,min}$, α_{err} and $\alpha_{err,man}$ as criteria, the kinetic model best describing a non-isothermal kinetic curve can be identified unambiguously.

Concurrent reactions

Theoretical curves, including up to as many as three kinetic models, can be constructed. The contribution of each of these models to the total simulated curve can be varied to obtain a total curve with $\alpha \in [0,1]$. A simulated curve describing a part of the experimental curve can be subtracted from the experimen-

tal data in order to obtain the remainder of the experimental curve for further analysis.

Software test using simulated curves as "experimental" data

If theoretical curves are simulated and used as "experimental" data and, therefore, as primary input to the kinetic software, the selectivity of the software in determining the appropriated mechanism can be evaluated.

A kinetic curve with the following parameters was simulated and used as input to the kinetic analysis software;

First-order rate equation:

$f(\alpha) = -\ln(1-\alpha)$ (F8, Table 1)

$E_a = 200.0$ kJ·mol^{-1}

$\ln A = 20.00$ (A reported in units of min^{-1})

$\varphi = 1$ deg·min^{-1}

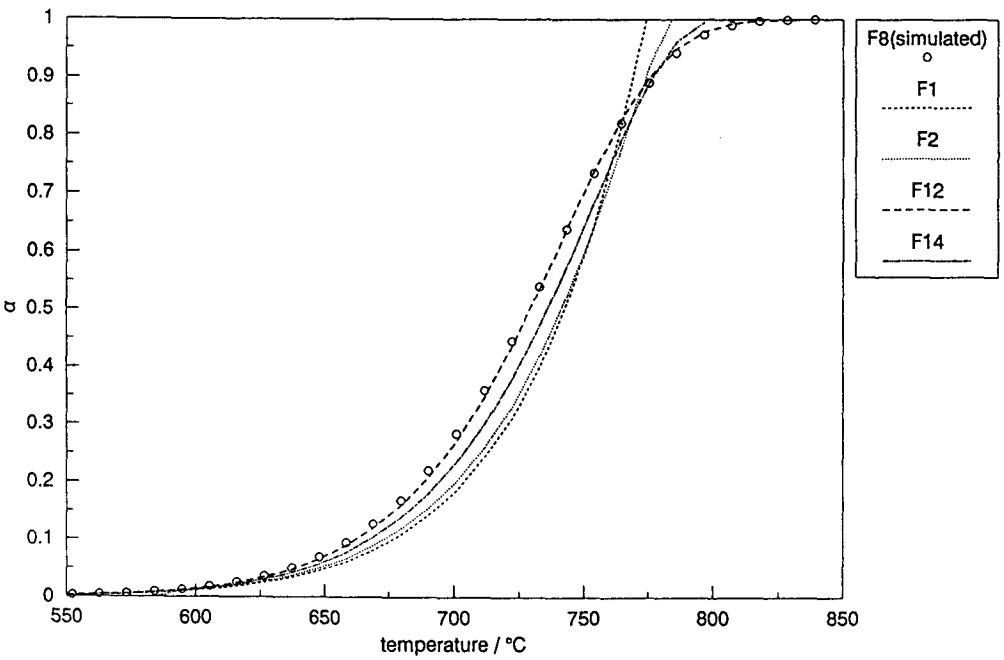

Fig. 1 Simulated non-isothermal kinetic curve with $f(\alpha) = -\ln(1-\alpha)$, $E_a = 200$ kJ·mol^{-1}, $\ln A = 20$ (A in min^{-1}) and $\varphi = 1$ deg·min^{-1}. The optimum description of some other functions are given for comparison

Table 2 Results obtained from analysis of the simulated First-order equation

Model number	E_a / kJ·mol^{-1}	ln$A$ (*)	$S_{B,min}$ / % of B	α_{err} / %	$\alpha_{err,max}$ / %	Ranking (**)			
			P_1	P_2	P_3	P_1	P_2	P_3	O
F1	374.4	39.86	1.71 (Y)	2.488	7.052	15	14	13	16
F2	377.0	39.69	1.42 (Y)	2.763	6.630	10	15	11	12
F3	170.9	15.16	2.59 (Y)	4.712	10.630	17	17	17	18
F4	381.0	38.97	0.99 (N)	2.208	5.713	8	13	8	9
F5	367.7	36.59	2.03 (Y)	3.427	7.338	16	16	16	17
F6	381.0	39.69	2.66 (N)	2.016	5.867	18	12	9	15
F7	310.8	32.77	0.77 (Y)	#	#	6	#	#	6
F8	200.0	20.00	0.00 (Y)	0.000	0.000	1	1	1	1
F9	128.8	11.17	0.02 (Y)	0.016	0.057	2	2	2	2
F10	93.3	6.68	0.05 (Y)	0.029	0.093	3	3	3	3
F11	58.1	2.11	0.10 (Y)	0.088	0.362	4	4	4	4
F12	40.2	–0.32	0.16 (Y)	0.146	0.621	5	5	5	5
F13	187.4	17.33	1.08 (Y)	1.104	4.626	9	7	7	8
F14	190.7	17.44	0.8 (Y)	0.831	3.416	7	6	6	7
F15	180.3	16.88	1.64 (Y)	1.511	7.063	13	9	15	13
F16	83.9	5.13	1.63 (Y)	1.535	7.054	12	11	14	13
F17	51.8	1.04	1.61 (Y)	1.516	6.857	11	10	12	11
F18	35.6	–1.13	1.65 (Y)	1.480	6.510	14	8	10	10
F19	140.9	16.39	8.81 (Y)	19.61	38.730	19	19	19	19
F20	298.8	39.55	9.30 (Y)	19.66	38.850	20	20	20	20

* Calculated from A in units of min $^{-1}$.** Ranking based on parameters P_1, P_2, P_3. The last column gives an overall ranking based on the three parameters

Due to the nature of this model, these parameters could not be calculated over the range $\alpha \in (0,1)$

(Y) or (N) indicates whether S_B has a global minimum value

Results of the analysis of this kinetic curve are summarized in Table 2. This table clearly indicates that the First-order model describes the "experimental" curve best. The differences between optimum description derived from different models are subtle (Fig. 1), but nevertheless distinguishable.

Various kinetic models have been simulated and used as "experimental" data. The criteria and ranking system used (Table 2), unambiguously leads to the appropriate mechanism. In each instance the simulated model had the lowest values of S_B, α_{err} and $\alpha_{err,max}$. This is contradictory to the findings of Criado *et al.* [19]. They showed that, with their simulation methods, various mechanisms lead to non-unique kinetic curves under non-isothermal conditions. For example, they showed that the Jander equation, F4 in Table 1, (with E_a = 308 kJ·mol^{-1} and ln A = 33.52 (A in min^{-1}) and the Avrami-Erofeev equation with n = 2, F10 in Table 1, (with E_a = 76 kJ·mol^{-1} and ln A = 6.58) define exactly the same kinetic curve. In this study it was found that these models are distinguishable. If the kinetic model F10, with the kinetic parameters used by Criado [19], was used as experimental data and the optimum fit for F4 was determined, values for E_a and ln A of 328 kJ·mol^{-1} and 34.58 respective were ob-

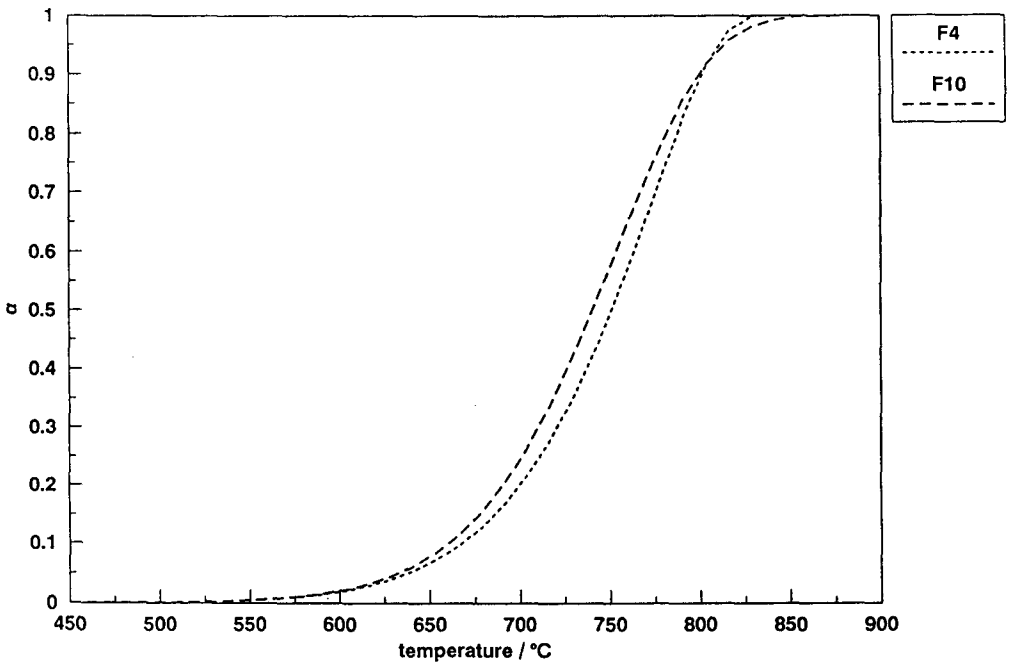

Fig. 2 Results obtained from analysis of F10 as experimental data in order to obtain an optimum description by F4

tained. These two curves are shown in Fig. 2, and they are distinctly different. It is therefore clear that the method used by Criado to simulate non-isothermal kinetic curves was not accurate enough and may lead to misconceptions about non-isothermal kinetic analysis.

The software may be used to study the effect of calculation errors on kinetic mechanisms and parameters. The primary input, i.e. temperature versus α data of a simulated curve, can be altered by introducing systematic errors in the input data and the effect of this on the kinetic curve can be investigated. Theoretical studies on the effect of overlapping reactions can also be investigated. Such studies are in progress at the moment.

Evaluation of the kinetic software by investigating the kinetics of the decomposition of $CaCO_3$

The kinetics of this reaction have been extensively studied. The contracting-area and contracting-volume rate laws proved to be applicable according to Gallagher and Johnson [20]. They compared the results of various investigations of this decompositions. This reaction, rather than a relatively uncharacterized reaction, was chosen to show that the method reported in this study leads to the appropriate mechanism.

Experimental

TG curves obtained using a Netzsch Simultaneous Thermal Analyser STA429. Both TG and DTA sample pedestals were used. Sample containers were of perforated, sintered alumina. Temperatures were measured with Pt-6% Rh/Pt-30% Rh thermocouples mounted directly below and touching the sample and reference crucibles. Four non-isothermal experiments were carried out in a dynamic Ar atmosphere (150 $cm^3 \cdot min^{-1}$). $CaCO_3$ samples (Riedel de Haen, minimum 99.0% purity) with masses varying between 49.0 and 53.9 mg were decomposed at heating rates of 2, 5, 10 and 20 $deg \cdot min^{-1}$. Six non-isothermal experiments were carried out in a static air atmosphere. $CaCO_3$ samples (10.7 to 500 mg) were decomposed at a constant heating rate of 20 $deg \cdot min^{-1}$. All samples were in an uncompressed powder form, except the 500 mg sample which was pelleted.

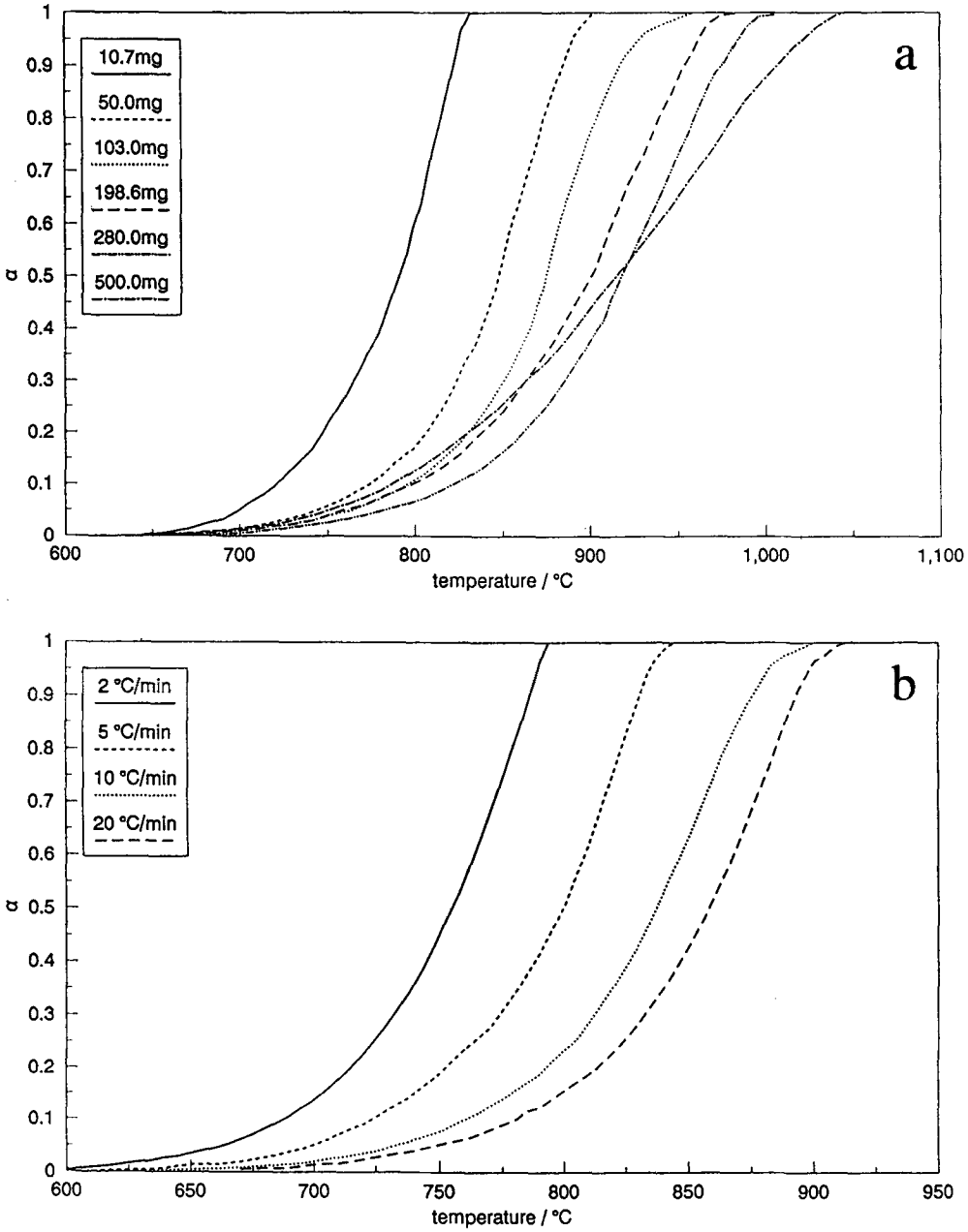

Fig. 3 Experimental α *vs.* temperature curves for the decomposition of $CaCO_3$ under varying conditions: (a) Ar (150 ml·min^{-1}), sample size: 49 to 53 mg, φ as indicated (b) Air (0 ml·min^{-1}), φ = 20 deg·min^{-1}, samples sizes as indicated

Table 3 Results obtained from analysis of the decomposition of 51.7 mg $CaCO_3$ in an Ar atmosphere at a heating rate of 2deg·min^{-1}

Model number	E_a / kJ·mol^{-1}	ln$A$ (*)	$S_{B,min}$ / % of B	α_{err} / %	$\alpha_{err,max}$ / %	Ranking (**)			
			P_1	P_2	P_3	P_1	P_2	P_3	O
F1	405.5	43.75	0.76 (Y)	0.823	6.829	12	6	14	11
F2	425.4	45.71	0.65 (Y)	0.708	2.625	3	4	2	2
F3	173.9	15.89	1.29 (Y)	1.288	2.870	17	11	5	12
F4	454.4	48.04	0.66 (Y)	1.015	2.846	4	9	3	4
F5	388.3	39.22	0.92 (Y)	1.093	7.900	16	10	17	17
F6	476.0	51.23	1.51 (N)	2.053	7.002	18	17	16	18
F7	476.0	52.46	0.84 (N)	#	#	15	#	#	15
F8	238.5	24.94	0.79 (Y)	1.604	4.548	14	15	8	14
F9	154.0	14.69	0.76 (Y)	1.599	4.550	12	14	9	13
F10	111.7	9.47	0.74 (Y)	1.579	4.460	11	13	7	10
F11	68.9	4.05	0.72 (Y)	1.450	3.933	9	12	6	9
F12	49.3	1.50	0.71 (Y)	1.606	4.838	8	16	12	16
F13	212.2	20.74	0.60 (Y)	0.676	2.257	1	2	1	1
F14	219.6	21.33	0.62 (Y)	0.943	2.856	2	8	4	3
F15	195.2	19.13	0.72 (Y)	0.839	6.939	9	7	15	8
F16	90.3	6.50	0.68 (Y)	0.679	4.582	5	3	10	5
F17	55.6	2.14	0.69 (Y)	0.738	5.004	6	5	13	7
F18	36.6	–0.38	0.70 (Y)	0.627	4.708	7	1	11	6
F19	214.4	24.31	3.86 (Y)	14.10	24.49	19	19	19	19
F20	452.2	55.06	4.06 (Y)	14.17	24.65	20	20	20	20

* Calculated from A in units of min^{-1}** Ranking based on parameters P_1, P_2, P_3. The last column gives an overall ranking based on the three parameters

Due to the nature of this model, these parameters could not be calculated over the range $\alpha \in (0,1)$

(Y) or (N) indicates whether S_B has a global minimum value

Results and discussion

Mechanism and kinetic parameters

The ten TG curves (Fig. 3) were analyzed using the developed software and a typical output is given in Table 3. The contracting-area and contracting-volume rate laws (F13 and F14 in Table 1) were found to be the models best describing the experimental data. A general observation was that the smaller the sample size, the better the contracting-area rate law (F13) described the experimental data, while at large sample sizes, the contracting-volume rate law (F14) proved more applicable. It is clear from Fig. 4 that the differences between the models best describing the experimental data are small. Nevertheless, the results of this method correspond with the results obtained by other workers using different approaches, of which that of Gallagher and Johnson [20] is but one example.

The variation of E_a and ln A as a function of φ is tabulated (Table 4) for the four kinetic curves obtained in an Ar atmosphere. Somasekharam and Kalpagham [17] found that constancy of A as a function of φ can be used as a crite-

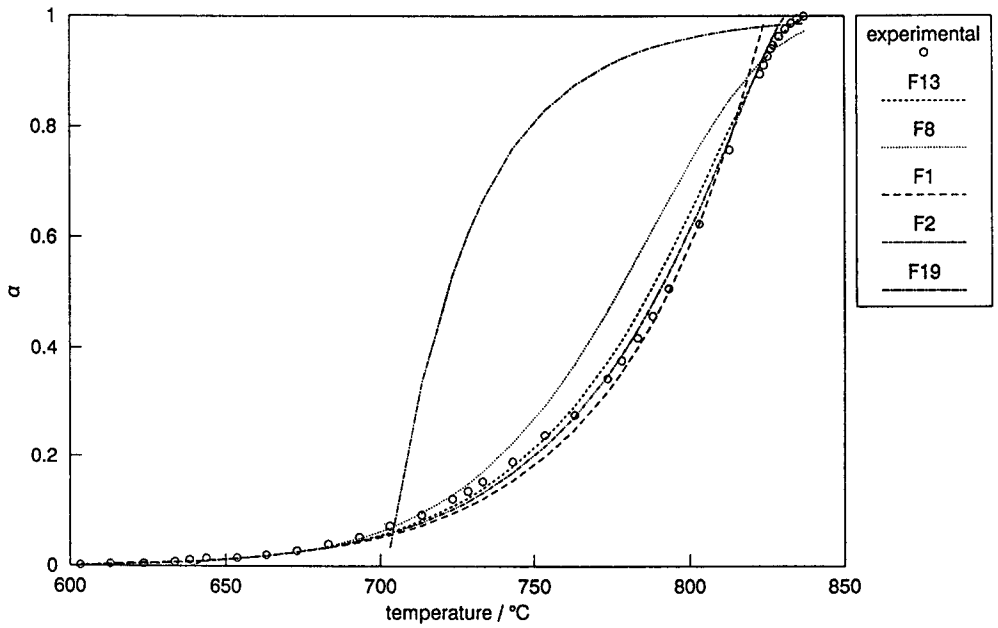

Fig. 4 Comparison between the experimental kinetic curve obtained when decomposing 53.0 mg $CaCO_3$ in Ar with $\varphi = 5$ deg·min^{-1} and the optimum description of this curve by simulated curves derived from the results of the kinetic analysis

rion in determining the model best describing the experimental data. The values listed in Table 4 support the findings of these workers. However, it must be realised that the kinetic parameters depend strictly on the experimental conditions used, and will only be similar if conditions such as mass, φ, atmosphere, density, sample preparation history, etc. are exactly similar. The results in Table 4 support the fact that the contracting geometry rate law is applicable to the decomposition of $CaCO_3$. The standard deviation, expressed as percentage of both the average E_a and the average ln A, is a minimum for the contracting-area kinetic model [F13].

Table 4 Constancy of E_a and ln A for the decomposition of 50 to 53 mg $CaCO_3$ in Ar at heating rates of 2, 5, 10 and 20 deg·min^{-1}

Model No.	E_a/kJ·mol^{-1}	σ/% of E_a	ln$A$	σ/% of ln$A$
F1	393.3	3.478	41.17	5.424
F2	415.0	2.610	43.19	4.879
F3	164.7	7.475	14.96	8.223
F4	448.0	2.567	45.86	4.880
F5	375.9	4.511	36.63	6.662
F6	*	*	*	*
F7	*	*	*	*
F8	238.2	4.320	24.72	5.795
F9	153.7	4.491	14.93	6.564
F10	111.3	4.524	9.92	7.908
F11	69.1	4.732	4.82	15.338
F12	48.8	5.470	2.29	30.470
F13	207.6	2.533	20.11	3.742
F14	216.1	2.697	20.80	4.250
F15	188.9	3.796	18.37	4.145
F16	86.6	4.992	6.63	3.759
F17	53.1	5.058	2.61	10.745
F18	35.7	5.022	0.41	121.280
F19	240.9	20.950	27.41	21.850
F20	437.6	11.560	52.71	13.110

*Values of E_a and ln$A$ not taken into account owing to the fact that S_B did not go through a minimum in the E_a range considered.

The average values of E_a (207.6 kJ·mol^{-1}) and ln A (20.11) for the decomposition of approx. 50 mg $CaCO_3$ in Ar (Table 4) are in good agreement with the

results of other investigations, which were reviewed by Gallagher and Johnson [20]. They calculated an activation energy of 187.1 kJ·mol^{-1} for a 50 mg sample in O_2 using the contracting-area rate law and isothermal methods of analysis. Their non-isothermal experiments lead to kinetic parameters of E_a = 215.4 kJ·mol^{-1} and ln A = 18.67 for a 15.87 mg sample at a heating rate of 0.29 deg·min^{-1}.

Correspondence between isothermal and non-isothermal kinetics

When isothermal kinetic curves are simulated using kinetic data obtained from non-isothermal kinetic software, it is clear that the contracting-geometry rate laws describe the experimental isothermal curve best (Fig. 5). In particular, the contracting-area rate law gives a good description of the experimental data. Most of the other models fail to describe the experimental curve adequately. If conditions such as atmosphere, sample size and others are kept the same under both isothermal and non-isothermal conditions, the appropriate mechanism and

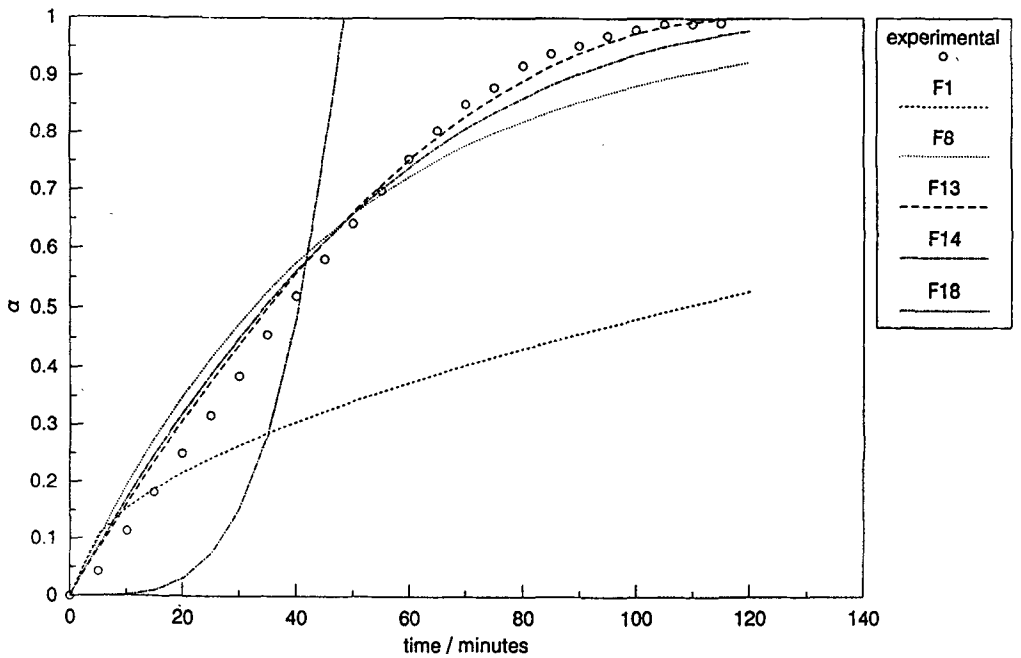

Fig. 5 Comparison between isothermal experimental data and simulated isothermal curves obtained by using F13, E_a = 207.6 kJ·mol^{-1} and ln A = 20.11. The experimental curves were obtained by decomposing 50 mg $CaCO_3$ in Ar (150 ml·min^{-1})

kinetic parameters, obtained form non-isothermal kinetic analysis, should indeed result in a good description of isothermal curves, as illustrated in Fig. 6.

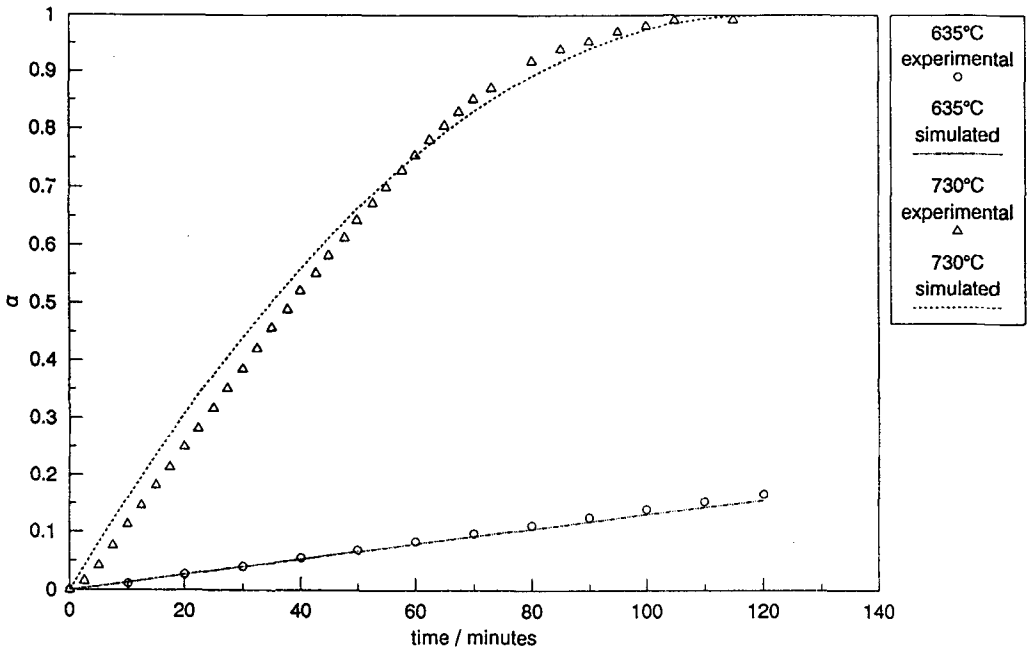

Fig. 6 Comparison between the isothermal kinetic curve, obtained when 50.0 mg $CaCO_3$ is decomposed in Ar (150 ml·min^{-1}) at 730°C, and the optimum descriptions for various kinetic models derived from non-isothermal kinetic analysis

Compensation effect (c.e.) in $CaCO_3$

The values of E_a and ln A, obtained under varying conditions, are represented in Fig. 7. A statistical analysis of the kinetic data obtained yielded the following linear equation:

$$\ln A = 0.135E_a - 7.92 \; (r = 0.994)$$

The value of k_{iso} is therefore 3.639×10^{-4} min^{-1} and the value of T_{iso} is 619°C. Gallagher and Johnson [20] used the method of Coats and Redfern [14] to determine the kinetic parameters for the decomposition of $CaCO_3$ in a dry oxygen atmosphere. The compensation parameters, obtained by using the contracting-area rate law and kinetic parameters from their investigation, are listed in Table 5.

Table 5 Compensation parameters according to the present study and that of Gallagher and Johnson [20] using different methods

Method	ln k_{iso}	$1/[RT_{iso}]$ / mol·kJ^{-1}	r	T_{iso} / °C	k_{iso} / min^{-1}
This study	–7.92	0.135	0.994	619	$3.63 \cdot 10^{-4}$
CR	–13.72	0.153	0.987	513	$1.10 \cdot 10^{-6}$
FC	–9.55	0.135	0.981	619	$7.12 \cdot 10^{-5}$
ABS	–13.85	0.153	0.977	513	$9.66 \cdot 10^{-7}$

CR – Coats and Redfern; FC – Freeman and Carroll; ABS – Achar, Brindley and Sharp

There has been a long enduring debate and discussions on the subject of the compensation effect in solid state reaction kinetics [21–26]. Agrawal [25] have pointed out the importance of the c.e. in solid state kinetics. He criticized [21] Zsakó and Arz [23] on their approach of using the linearity of the plot of ln A as a function of E_a to determine the compensation parameters and to establish whether or not the reaction under consideration displays the compensation ef-

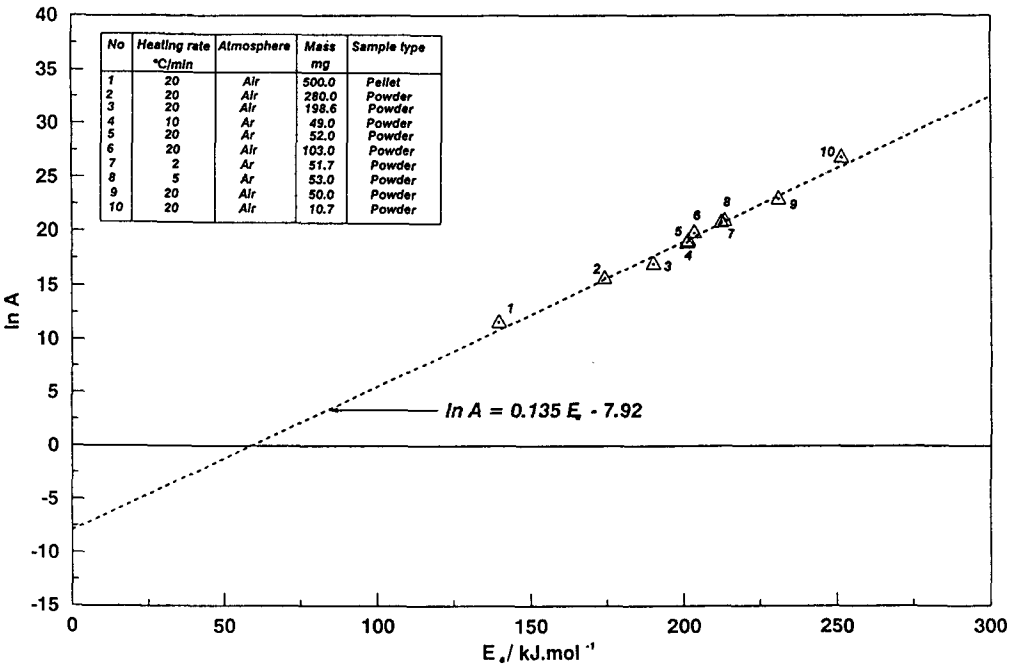

Fig. 7 Conventional plot for the decomposition of $CaCO_3$, obtained when using the contracting-area rate law (F13). Conditions and the corresponding results are indicated

fect. Agrawal argued that, although Zsakó and Arz observed a straight line fit of ln A as a function of E_a for the decomposition of $CaCO_3$, the Arrhenius plots of all data used by Zsakó and Arz showed no common point of intersection. (This will also be the case in the present study because of the fact that the standard deviation of the compensation line does not equal one.) There is some justification in the arguments of Agrawal [21] because of the fact that the Arrhenius plot is more sensitive than the conventional compensation effect plot. However, if the criterion of Agrawal is to be used to determine the c.e., very few reactions will ever show the so-called real compensation effect. It must be realized that all experimental measurements (and in particular thermal analysis measurements) are subject to some degree of error, and therefore the correlation coefficient of the conventional c.e. plot (ln A *vs.* E_a) will never equal one. As Zsako and Somasekharam [24] showed, only an exact straight line of ln A as a function of E_a will result in T_{iso} having a standard deviation of zero.

The criticisms of Agrawal [21] only indicates that the compensation effect of $CaCO_3$ have not been characterised very well by Zsakó and Arz [23]. A possible reason for this is the fact that the values of E_a and A reported by Zsakó and Arz [23] were calculated from varying values of the reaction order (n). The data in Fig. 7 indicate true compensation effect for the decomposition of $CaCO_3$.

Conclusions

The subject of solid state-state kinetics is one of many controversies. A good example of this is the fact that the thermal decomposition of $CaCO_3$, a relatively simple reaction, has been studied extensively and yet, almost every investigation leads to different kinetic parameters, stimulating more investigations which leads to yet more unique results.

One point of controversy cleared up in the paper is that non-isothermal kinetic analysis, as carried out in this investigation, can be selective in the determination of reaction mechanisms and subsequently the correct kinetic parameters.

Maciejewski [27] pointed out the problems of kinetic analysis and stated that well-elaborated computer programs are necessary to solve for kinetic parameters. It is believed that the software described in this paper provides a very accurate path for solid-state kinetic analysis.

* * *

This work is published by the permission of the Council for Mineral Technology (MINTEK).

References

1 J. Sestak, Talanta, 13 (1966) 567.
2 J. H. Sharp and S. A. Wentworth, Anal. Chem., 41 (1969) 2060.
3 P. M. D. Benoit, R. G. Ferrillo and A. H. Granzow, J. Thermal Anal., 30 (1985) 869.
4 J. M. Criado, M. Gonzales, A. Ortego and C. Real, J. Thermal Anal., 34 (1988) 1387.
5 H. Tanaka and N. Koga, J. Thermal Anal., 34 (1988) 685.
6 E. Koch, J. Thermal Anal., 33 (1988) 1259.
7 J. Sestak, J. Thermal Anal., 33 (1988) 1263.
8 I. Agherghinei, J. Thermal Anal., 34 (1988) 909.
9 C. D. Doyle, J. Appl. Polym. Sci., 15 (1961) 285.
10 J. Zsakó, J. Thermal Anal., 2 (1970) 145.
11 G. Gyulai and E. J. Greenhow, Thermochim. Acta 6 (1973) 239.
12 K. N. Ninan, J. Thermal Anal., 35 (1989) 1267.
13 G. Gyulai and E. J. Greenhow, J. Thermal Anal., 6 (1974) 279.
14 A. W. Coats and J. P. Redfern, Nature, 201 (1964) 68.
15 H. H. Horwitz and G. Metzger, Anal. Chem., 35 (1963) 1464.
16 J. R. MacCullum and J. Tanner, Eur. Polym. J., 6 (1970) 1033.
17 K. N. Somasekharam and V. Kalpagam, J. Thermal Anal., 34 (1988) 777.
18 J. Zsakó, J. Phys. Chem., 72 (1968) 2406.
19 J. M. Criado, A. Ortego and F. Gotor, Thermochim. Acta, 157 (1990) 171.
20 P. K. Gallagher and D. W. Johnson, Thermochim. Acta, 6 (1973) 239.
21 R. Agrawal, J. Thermal Anal., 31 (1986) 73.
22 J. Zsakó, J. Thermal Anal., 5 (1973) 239.
23 J. Zsakó and H. E. Arz, J. Thermal Anal, 6 (1974) 651.
24 J. Zsakó and K. N. Somasekharam, J. Thermal Anal., 32 (1987) 1277.
25 R. Agrawal, J. Thermal Anal., 34 (1988) 1141.
26 R. Agrawal, J. Thermal Anal., 35 (1989) 909.
27 M. Maciejewski, J. Thermal Anal., 33 (1988) 1269.

Zusammenfassung — Unter Anwendung der Zsakó Methode können kinetische Parameter und Mechanismen von Feststoffreaktionen aus einem einzigen nichtisothermen Experiment ermittelt werden. Diese Methode wurde computerisiert und bei theoretischen und praktischen Untersuchungen sowie bei der Separierung von überlappenden Reaktionen angewendet.